Applied Surface Science 316 (2014) 308–314

Contents lists available at ScienceDirect

Applied Surface Science

journal homepage: www.elsevier.com/locate/apsusc

One step synthesis of polyacrylamide functionalized graphene and its application in Pb(II) removal

Zhiwei Xu, Yaoyao Zhang, Xiaoming Qian, Jie Shi, Lei Chen, Baodong Li, Jiarong Niu, Liangsen Liu*

Key Laboratory of Advanced Braided Composites, Ministry of Education, School of Textiles, Tianjin Polytechnic University, Tianjin 300387, People's Republic of China

ARTICLE INFO

Article history:
Received 27 April 2014
Received in revised form 18 July 2014
Accepted 24 July 2014
Available online 2 August 2014

Keywords:
Graphite oxide
Polyacrylamide
γ-Ray irradiation
Lead adsorption
Functionalized graphene
Heavy metal

ABSTRACT

Polyacrylamide grafted graphene (PAM-g-graphene) from graphite oxide (GO) was successfully prepared by γ-ray irradiation with acrylamide monomers in aqueous at room temperature in this paper. Our strategy involves the PAM chains graft on the surface and between the layers of GO by in situ radical polymerization which led to the exfoliation of GO into individual sheets. Results show that the degree of grafting of PAM-g-graphene samples is 24.2%, and the thickness is measured to be 2.59 nm. Moreover, the as-prepared PAM-g-graphene with some amino from PAM and little oxygen functional groups exhibit superior adsorption of Pb(II) ions. The adsorption processes reach equilibrium in just 30 min and the adsorption isotherms are described well by Langmuir and Freundlich classical isotherms models. The determined adsorption capacity of PAM-g-graphene is 819.67 mg g^{-1} (pH 6) for Pb(II), which is 20 times and 8 times capacities of that for graphene nanosheets and carbon nanotubes according to reports, respectively. This chemically modified graphene synthesized by this fast one-step approach, featuring a good versatility and adaptability, excellent adsorption capacity and rapid extraction, may provide a new idea for the global problem of heavy metal pollutants' removal in water.

1. Introduction

Graphene, a single-layer carbon sheet with a hexagonal packed lattice structure, exhibits many unique properties such as high values of Yong's modulus, fracture strength, thermal conductivity, specific surface area, and electrical conductivity [1–4]. Therefore, it exhibits great potential applications in many technological fields such as field-effect transistors, solar cell, sensor, supercapacitors, composites and transparent electrodes [4–9]. The superior properties of graphene compared to polymers are also reflected in polymer/graphene nanocomposites [7]. Graphene-based polymer composites show superior mechanical, thermal, gas barrier, electrical and flame retardant properties, compared to the neat polymer [10,11]. Graphene and graphene-based polymer nanocomposites are important additions in the field of nanoscience. However, graphene tends to aggregate in solution and in the solid state, giving rise to a great technical difficulty in the fabrication of graphene-based devices by spin- or blade-coating a solution in organic solvent [12]. In order to overcome these problems, functionalization and dispersion of graphene sheets are of crucial importance for their end applications.

Graphite oxide (GO) is a layered material produced by the oxidation of graphite. GO consists of intact graphitic regions interspersed with sp^3-hybridized carbons containing hydroxyl and epoxy functional groups on the top and bottom surfaces of each sheet and sp^2-hybridized carbons containing carboxyl and carbonyl groups mostly at the sheet edges [13,14]. So a great variety of chemical reactions can occur between the single functionalized molecule and the functional groups existing in GO structure. The complete exfoliation of GO in various solvents followed by the polymer covalently grafted to the reactive oxygen functionalities by in situ polymerization would be a promising route to achieve mass production of chemical modified graphene platelets.

γ-Ray possesses the shortest wavelength, highest energy and a much greater penetrating distance through material atoms due to its zero charge and mass [15]. γ-Ray irradiation has been extensively investigated as a scalable, simple and cost-effective technique to control the properties of carbon systems [16–18]. In former researches, some investigators have proved the reduction effect to graphene oxide during the γ-ray irradiation. Youwei Zhang et al. reported the approach to prepare well-dispersed graphene sheets by γ-ray induced reduction of a graphene oxide suspension

* Corresponding author. Tel.: +86 022 83955231; fax: +86 022 83955231.
E-mail address: 83019163@163.com (L. Liu).

http://dx.doi.org/10.1016/j.apsusc.2014.07.155
0169-4332/

in *N*,*N*-dimethyl formamide at room temperature [3]. Bowu Zhang et al. reported the effect of γ-ray irradiation on the reduction of graphene oxide sheets in alcohol/water system and propose the mechanism of radiation-induced reduction of graphene oxide in alcohol/water. The reductive radicals produced in the mixture solvent can be used to create a reducing medium for chemical reaction under the γ-ray irradiation in the absence of oxygen [4]. In addition, this radiation-induced functionalization is one of the most effective techniques because of its uniform creation of radical sites in the respective polymer matrix [19–21]. Moreover, radiation-induced graft polymerization is versatile for vinyl monomers which undergo free radiation polymerization, and production can be easily scaled-up [18,22]. For example, Yang et al. performed the functionalization of multiwalled carbon nanotubes by radiation-induced graft polymerization of vinyl monomers in aqueous solution at room temperature with the desired functional group using γ-ray irradiation [22]. Lee et al. provided a controllable way to prepare hydrogels based on chemical bonds between the graphene oxide sheets and polymer via a γ-ray pre-irradiation technique [23]. We have previously published research regarding the GO interlayer functionalization before exfoliation, and prepared functionalized graphene nanosheets with the potential order of intercalation, grafting and exfoliation of GO by a one-step γ-ray irradiation protocol [17]. Therefore, this simple and fast one-step method would be a candidate of scalable way for functionalized graphene from GO.

Removal of toxic metals is one of the biggest challenges in ensuring safe water for all as well as protecting the environment [24–26]. Lead is the most notorious metal ion found in water with toxicological and neurotoxical natures (brain damage) [27]. At higher concentration than permissible limit, lead will cause mental retardation, kidney disease and anaemia, etc. [5]. Long term drinking water containing high level cadmium can cause some disorders such as diarrhea, nausea, muscular cramps, renal degradation, lung insufficiency and cancer [28]. To tackle this problem, some methods have been developed for the removal of pollutants from water. These are based on physical, chemical, electrical, thermal and biological principles. The important methods are screening, filtration and centrifugation, micro- and ultra filtration, crystallization, sedimentation and gravity separation, flotation, precipitation, coagulation, oxidation, solvent extraction, evaporation, distillation, reverse osmosis, ion exchange, electrodialysis, electrolysis, adsorption [24–28], and so forth. In these technologies, adsorption is considered to be high efficiency, cost-effectiveness, simple operation, and environmental friendliness [29], and it is significant to exploit simple, novel and high efficient adsorbents for this approach.

Recently, graphene with super large surface area (2630 $m^2\ g^{-1}$) and flat structure can be used as an excellent adsorbent [30–32]. However, the use of graphene for the applications like wastewater adsorption is limited. This mainly results from its difficulty in preparing composites with other materials because the surface of a graphene sheet has little reactive groups [12,31]. Therefore the reactive groups on the surface of graphene oxide provide a good compatibility with polymers and form a graphene oxide/polymer composite with a stable structure [30,32–34]. Considering the abundant oxygenic groups, the adsorption presumably occurs on the surface of graphene oxide/polymer nanocomposites when graphene oxide/polymer nanomaterials were used as an adsorbent for removal of heavy metal ions from aqueous solutions. Up to now, graphene oxide and its composites have been applied in the adsorption of heavy metal ions, such as Au(III), Pt(IV), Cu(II), Cd(II), Pb(II), Zn(II) and Hg(II) ions [5,30,33–36]. These effective adsorbents with strong hydrophilicity, huge specific surface area, and a particular nanosheet structure could improve their adsorption capacity.

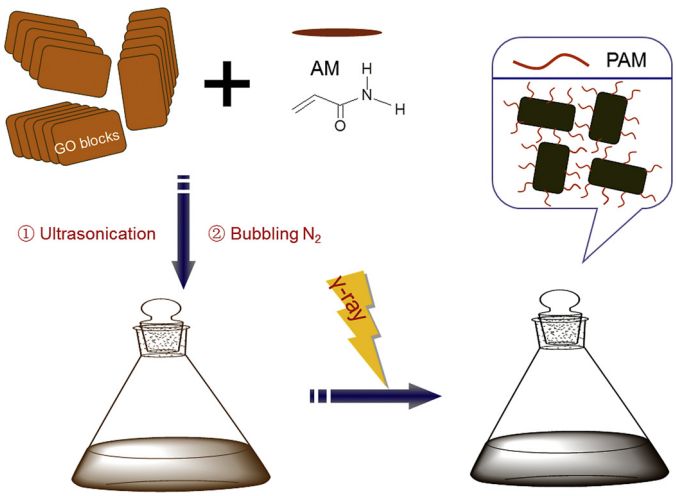

Scheme 1. Schematic of the synthesis of PAM-g-graphene by the γ-ray irradiation.

In this work, we have presented and discussed the results concerning the effect of γ-ray treatment of graphite oxide and acrylamide (AM). Our strategy involves the PAM chains graft on the surface and between the layers of GO by in situ radical polymerization which led to the exfoliation of GO into individual sheets, and the γ-ray induced reduction further to produce the functionalized graphene sheet simultaneously. The characteristics results of UV–vis absorption, Fourier transform infrared spectroscopy (FTIR), X-ray photoelectron spectroscopy (XPS), X-ray diffraction (XRD), thermogravimetric analysis (TGA) and atomic force microscopy (AFM) analyses showed that PAM-g-graphene is synthesized by the co-irradiation between GO and AM monomers in water at room temperature. The sample was firstly degassed overnight at 120 °C, and then the obtained N_2 adsorption–desorption isotherms were evaluated to give the N_2-BET specific surface area (SSA). The formation of the PAM-g-graphene with some amino, little oxygen functional groups would be a new polymer composite for the removal of heavy metals from industrial wastewater. Consequently, we investigate its ability to treat wastewater that contains Pb(II) ions. In a controlled experiment, we used the GO to perform the adsorption experiment using the same procedure. The adsorption ability of Pb(II) by pristine, oxide, chitosan, electrolysis modified graphene and graphite oxide is compared. This chemically modified graphene synthesized by this fast one-step approach, featuring a good versatility and adaptability, excellent adsorption capacity and rapid extraction, may provide a new idea for the global problem of heavy metal pollutants' removal in water.

2. Materials and methods

2.1. PAM-g-graphene preparation

GO was prepared following the improved Hummers method and subsequently freeze-dried for 48 h to obtain GO blocks. Then freshly-prepared GO blocks (250 mg) and acrylamide (500 mg) were mixed in 100 ml deionized water and sonicated for 30 min to disperse the solids homogeneously. The resultant mixture was deoxygenated by bubbling high-purity nitrogen for 15 min and then irradiated with the absorbed doses of 300 kGy (dose rate: 0.8 $kGy\ h^{-1}$) by γ-ray under atmospheric pressure and ambient temperature. The preparation of PAM-g-graphene composite is schematically shown in Scheme 1. After irradiation, the grafted GO was purified by cycling centrifugate/deionized water-redispersion, until no absorption peaks appeared by the UV–Vis spectrum of the supernatant for the resultant mixture. The obtained

PAM-g-graphene was freeze-dried for 24 h and vacuum dried at 50 °C for 12 h later. The preparation process was systematically investigated by UV–Vis spectrum, FTIR XPS and XRD. The degree of grafting (DG) was estimated by TGA for the GO and PAM-g-graphene and was calculated using Eq. (1):

$$\mathrm{DG}(\%) = \frac{R_G - R}{R_G - R_P} \times 100\% \quad (1)$$

Wherein, R_G, R and R_P represent the residual weight percentage (wt%) of GO, and PAM-g-graphene, PAM pyrolysis, respectively.

2.2. Adsorption experiments

Adsorption tests of Pb(II) ions on PAM-g-graphene at varying adsorption time and initial Pb(II) ion concentration were carried out by a batch method. For the batch adsorption experiments, about 1 mg PAM-g-graphene is added to 10 mL of Pb(II) aqueous solution with the desired concentration at pH 6.0 ± 0.1. To facilitate thorough mixing, we mildly stirred the solution for 120 min, and then the adsorption proceeded under static conditions at 293 K for 24 h to reach equilibrium. After a desired adsorption period, the solid was separated from the solution by centrifugation, and then the concentration of Pb(II) ions after adsorption was measured by ICP-MS analysis. In a controlled experiment, we used the GO to perform the adsorption experiment using the same procedure. The adsorption isotherm was obtained by changing the concentration of Pb(II) solution in the range of 5–100 mg L^{-1} and repeating the experiment under similar conditions. The amounts of Pb(II) ions were calculated from the difference between the initial concentration (C_0, mg g^{-1}) and the equilibrium one (C_e, mg g^{-1}) (Sorption % = $(C_0 - C_e)/C_0 \times 100\%$, and $C_s = (C_0 - C_e)/m \times V$, where C_s is the concentration of metal ion adsorbed on adsorbent, V is the volume of the suspension (L), and m is the mass of adsorbent (g)).

3. Results and discussion

3.1. Synthesis and characterization of materials

The chemical change from GO to PAM-g-graphene is confirmed by UV-vis absorption in Fig. 1(a). From the digital picture of GO and PAM-g-graphene dispersions in water, the color of GO dispersion changes from light brown to black after γ-ray irradiation with AM. As it is clearly seen, this increased absorption in the visible region is to be expected if reduction succeeds and aromatisation is enhanced [37]. In addition, the PAM-g-graphene dispersions in water is stable for 24 h, which further suggests that some of the hydrophilic PAM chains are grafted onto the GO sheets during the polymerization of AM. In water, the spectrum of GO dispersion presents two characteristic features: a maximum at 230 nm, corresponding to π–π* transitions of aromatic C-C bonds, and a shoulder around 300 nm, assigned to n-π* transition of C=O bonds [21,37]. After formation of PAM-g-graphene via γ-ray irradiation, the peak of PAM-g-graphene is observed at 260 nm. The maximum of the band assigned to aromatic bond has red-shifted to 260 nm, and this is attributed to the electronic conjugation within PAM-g-graphene restored by the γ-ray irradiation-induced grafting of PAM [38,39].

XRD was an important tool to understand how the entry of the functional groups affects graphene interlayer spacing via the γ-ray irradiation [40]. Fig. 1(b) shows the XRD patterns of GO and the as-prepared PAM-g-graphene by irradiation. GO powder shows a sharp peak at around $2\theta = 10.7°$, corresponding to the (0 0 1) reflection, which indicates that the interlayer space (0.82 nm) is much larger than that of pristine graphite (0.34 nm) due to the introduction of oxygen-containing functional groups on the graphite sheets. After PAM chains were introduced onto the GO sheets, the XRD peak of PAM-g-graphene was hardly observed, indicating that the PAM-g-graphene has been exfoliated effectively during the in situ polymerization induced by the γ-ray irradiation. Compared with GO, the intensity of (0 0 1) peak disappears in the XRD pattern for PAM-g-graphene, revealing that most of the PAM chains intercalated into the interlayer of GO, which promote the exfoliation of GO sheets. The functional groups in the surface and between the layers of GO have been evidenced by UV–vis absorption in Fig. 1(a) and the following analysis.

The conclusion is also authenticated by XPS analysis. As shown in Fig. 1(c), the intensity of the peak corresponding to sp^2-hydridized carbon located at 284.4 eV continually increases from GO to PAM-g-graphene, while the change of oxygen content shows the opposite trend. GO shows C/O mole ratio of 1.9 and this value increases to 10.3 after irradiation with AM, which indicate the elimination of most functional groups and the slight reduction of graphene sheets. It should be noticed that PAM-g-graphene exhibits nitrogen content as 3.1%, which further confirms the PAM functionalization on the surfaces of graphene. Additionally, in the C1s spectra of PAM-g-graphene (Fig. 2(d)), the binding energy of 284.4 eV is attributed to the C–C, C=C, and C–H bonds and the peak appears at 288.4 eV is assigned to the O=C–N of PAM [29,37]. It also proves the presence of PAM groups in the perapared functionalized graphene nanosheets.

This study used FTIR spectra for the qualitative chemical analyses of functional groups grafted on GO. From the spectrum of GO (Fig. 1(b)), the peak at 3400 cm^{-1} was according to the -OH vibration stretching. It also showed bands due to carboxyl C=O (1736 and 1630 cm^{-1}) and C-O (1390 cm^{-1}), epoxy C–O (1228 cm^{-1}) and alkoxy C–O (1054 cm^{-1}) groups situated at the edges of the GO nanosheets [41,42]. The disappearance of moiety characteristic peaks of oxide groups in PAM-g-graphene indicates that GO has been partially reduced to graphene. In the spectrum of PAM-g-graphene, the new emerging peak could be observed at 3200 cm^{-1}, corresponding to the –NH stretching of the PAM unit [41]. The absorption band at 2937 cm^{-1} can be assigned to the PAM asymmetric stretching vibration of C-H [42]. The peak around 1662 cm^{-1} and 1605 cm^{-1} is ascribed to the in-plane deformation vibration of N-H bond [38]. So the FTIR spectra suggested the successful grafting of PAM onto GO to form PAM-g-graphene and some reduction effect of γ-ray irradiation on GO.

TGA was used to evaluate the content and species of polymer attached onto GO shown in Fig. 1(f). For GO, the mass loss in the range of 100 to 200 °C is about 38.67%, attributed to the decomposition of labile oxygen [42,43]. For PAM-g-graphene, the first weight loss about 10% occurred from 50 to 100 °C as a result of moisture loss of the grafted hydrophilous PAM, and the second weight loss in the range 200–600 °C was due to the pyrolysis of the labile oxygen-containing functional groups and the grafted PAM moieties [41]. The mass loss of PAM-g-graphene was 51.03%, which indicating the decrease of thermally stable to PAM-g-graphene. Assuming the grafted polymer chains were completely pyrolyzed, the weight percentage of grafted PAM chains was as high as 24.2 wt%, as calculated according to Eq. (1).

The N_2-BET specific surface areas of the GO and PAM-g-graphene are 46.4 and 128 m^2 g^{-1}, respectively. The amino and little oxygen functional groups in PAM-g-graphene were easily reacted with carboxyl in another GO flake, which should result in the agglomerations of PAM-g-graphene. Moreover the samples were degassed overnight at 120 °C for SSA measurements. Since PAM-g-graphene powders tend to aggregate together, the SSA is normally lower than the theoretical value, and gas adsorption gives a much lower SSA value than that of liquid adsorption (the stable colloidal suspensions of GO and PAM-g-graphene). It is reasonable that the N_2-BET surface area of PAM-g-graphene is relatively lower. Thus, the introduction of PAM chains with functional groups to the

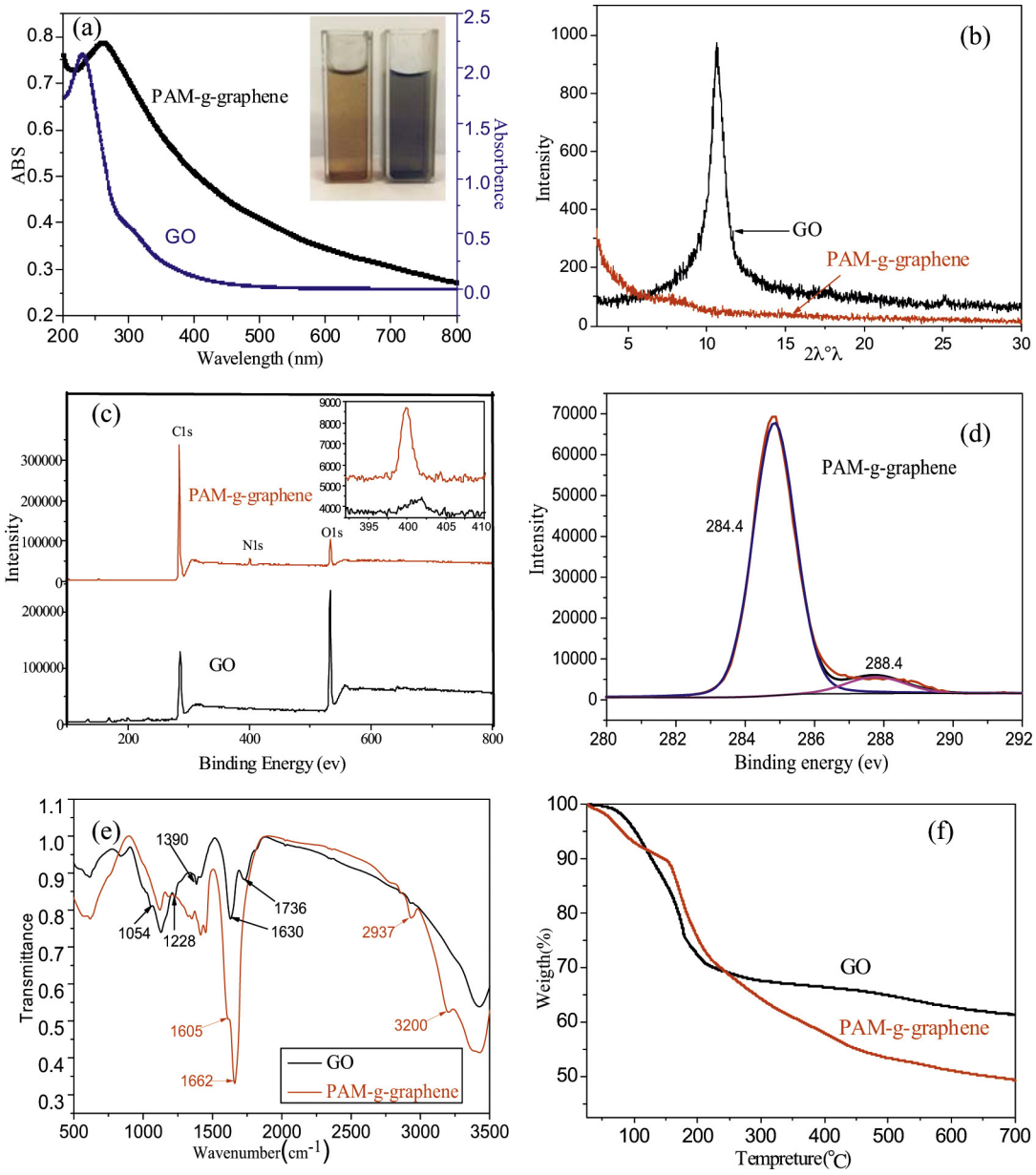

Fig. 1. (a) UV–Vis spectra of GO and PAM-g-graphene. The insert shows the photographs of GO (left) and PAM-g-graphene (right) dispersion in water after 24 h, (b) XRD patterns of GO and PAM-g-graphene, (c) XPS full-scan spectra for GO and PAM-g-graphene. The insert shows the nitrogen atom for GO and PAM-g-graphene, (d) XPS C1s spectra of PAM-g-graphene, (e) FTIR spectra of GO and PAM-g-graphene, (f) TGA curves (in N_2) of GO and PAM-g-graphene with a heating rate of 5 °C min^{-1}.

surface and interlayers of GO sheets is the main reason to increase the adsorption capacity of PAM-g-graphene for heavy metal.

The morphology of the prepared PAM-g-graphene is studied using AFM. As shown in Fig. 2(a–d), cross-sectional AFM analyses were conducted to investigate the structural features of GO sonicated for 2 h and PAM-g-graphene sheets dispersed in water. As can be seen in Fig. 2(b), many free-standing sheets with morphology similar to that of graphene oxide (Fig. 2(a)) and with sizes ranging from 500 nm to several micrometers are observed. From the cross-section analysis, we could find that the thicknesses of pristine GO single-layer sheets we prepared (~1.30 nm) are mostly a little higher than that reported, which is resulted from the extensive oxidation in the preparation procedure, matching well with the analysis of XRD. It should be noted that the thickness of the PAM-g-graphene nanosheets is measured to be 2.59 nm, which is higher than the pristine GO sheets. The AFM results show good agreement with the above analyses, further implying that the exfoliated functionalized graphene has prepared via γ-ray induced PAM chains interlayer graft on GO by in situ radical polymerization.

3.2. Absorption of Pb(II) on PAM-g-graphene

3.2.1. Effect of contact time on the adsorption

The experiment about the effect of contact time on the adsorption of Pb(II) onto PAM-g-graphene was executed using the metal ions concentration of 45 mg L^{-1} at pH 6 for Pb(II). Fig. 3(a) shows the kinetic curves of Pb(II) adsorbed onto PAM-g-graphene. It can be seen that the adsorption of Pb(II) onto PAM-g-graphene increases sharply within the first 20 min, and then it rises slowly and reaches equilibrium in 30 min. The process of adsorption achieved equilibrium in such a short time, suggested that PAM-g-graphene has very high adsorption efficiency and high-value industrial applications.

The kinetic of Pb(II) adsorption was determined in order to understand the adsorption behavior of the PAM-g-graphene. The

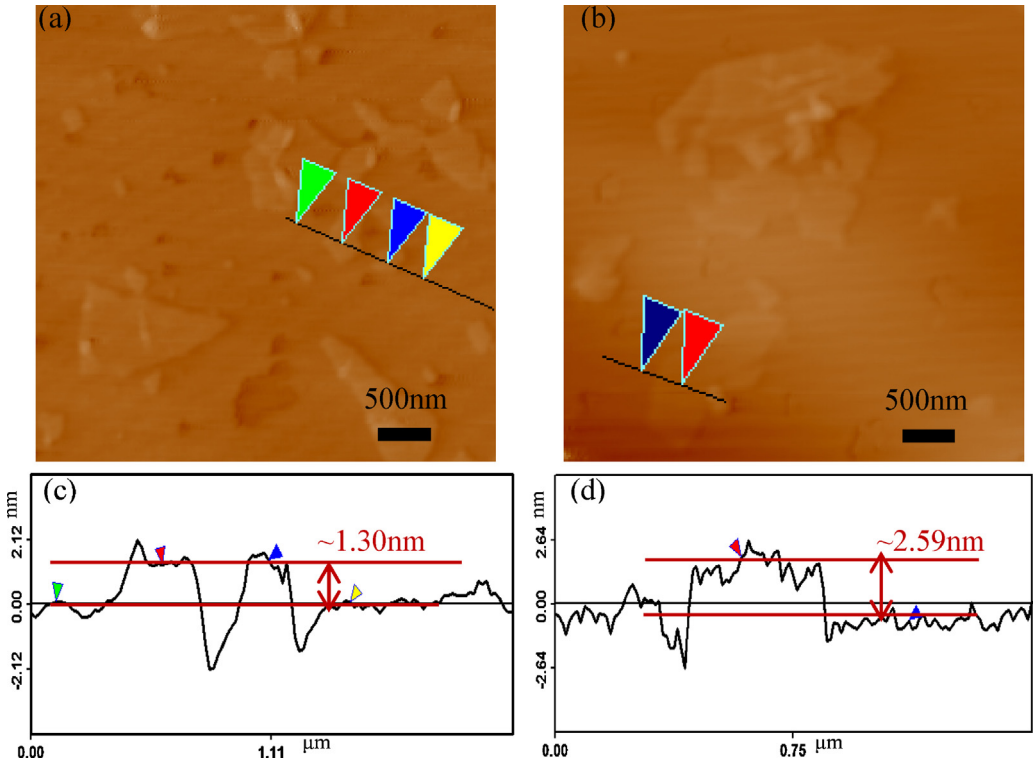

Fig. 2. Tapping mode AFM topographic images of (a) graphene nanosheets from the GO sonicated for 2 h, (b) graphene nanosheets from the dispersed PAM-g-graphene in water, (c) cross-section of graphene nanosheets from the sonicated GO and (d) cross-section of graphene nanosheets from the dispersed PAM-g-graphene in water.

pseudo-second-order kinetic model was expressed as following formulation (Eq. 2) [28]:

$$\frac{t}{q_t} = \frac{1}{K_2 q_e^2} + \frac{t}{q_e} \quad (2)$$

where K_2 is the pseudo-second-order rate constant ($g\,mg^{-1}\,min^{-1}$)). The values of q_e ($mg\,g^{-1}$) and K_2 can be gained from the slopes and the intercepts of the t/q_t versus t (min) plots.

It can be concluded from the kinetic models parameters presented in Fig. 3(b) that the adsorption process of Pb(II) on PAM-g-graphene is in accordance with the pseudo-second-order model. Moreover, the experimental q_e values (440.4 $mg\,g^{-1}$) are closer to q_e values calculated (458.7 $mg\,g^{-1}$) from the pseudo-second-order kinetic model. The correlation coefficient value ($R^2 = 0.999$) of pseudo-second-order kinetic model for the adsorption of Pb(II) suggests that the adsorption process of Pb(II) on PAM-g-graphene may be controlled by chemical adsorption involving valence forces through sharing or exchange electrons between sorbent and sorbate.

3.2.2. Adsorption isotherms

The Langmuir and Freundlich isotherm models are conventional models among the abundant isotherm models, and the adsorption isotherm models are used to fit experiment data usually and help to explore the adsorption mechanism much deeply. The Langmuir isotherm describes a homogeneous monolayer adsorption meaning all the adsorption sites have equal adsorbate affinity, and is expressed as Eq. (3) [44,45]:

$$\frac{C_e}{Q} = \frac{1}{K_L Q_0} + \frac{C_e}{Q_0} \quad (3)$$

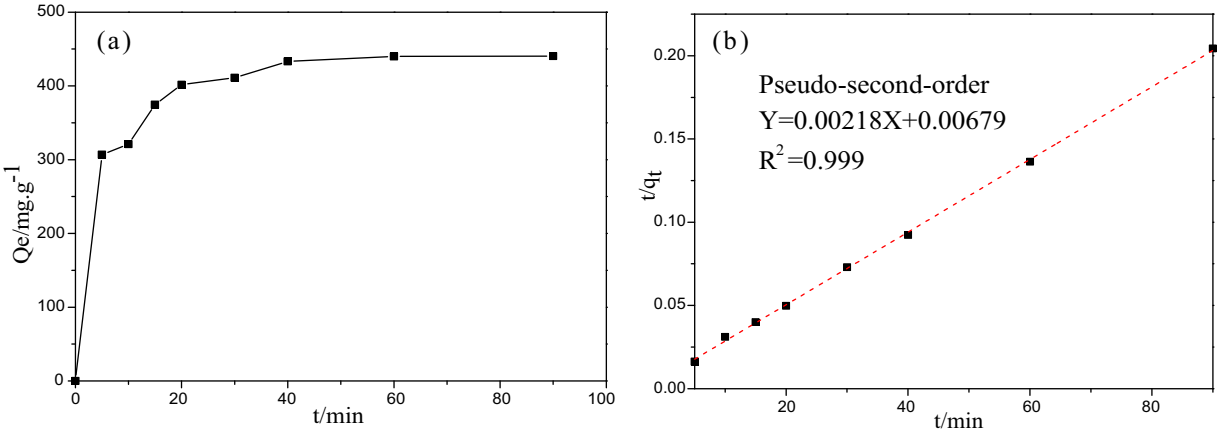

Fig. 3. Effects of contact time on adsorption of Pb(II) on removal efficiency by PAM-g-graphene (a) and the pseudo-second-order kinetics (b).

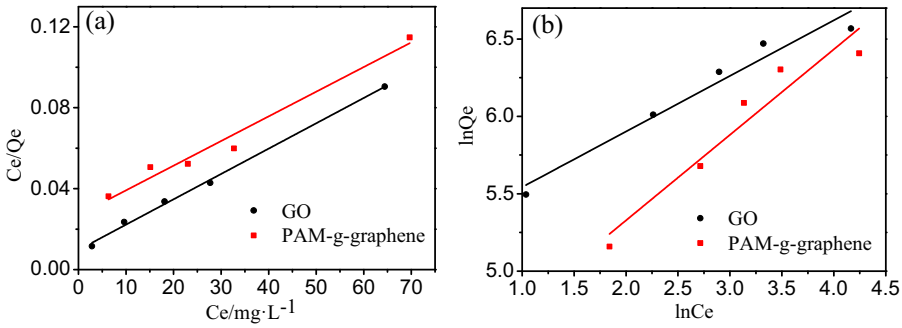

Fig. 4. (a) The Langmuir isotherm; (b) the Freundlich isotherm for the adsorption of Pb(II) onto the PAM-g-graphene and GO at 293 K.

Table 1
A comparison results between two isotherm models for Pb(II) adsorption on PAM-g-graphene and GO.

	Langmuir parameters			Freundlich parameters		
	Q_0 (mg g^{-1})	K_L (L mg^{-1})	R^2	K_F (L g^{-1})	n	R^2
PAM-g-graphene	819.67	0.045	0.9657	54.60	1.816	0.9057
GO	604.00	0.129	0.9964	178.25	2.782	0.9474

On the other hand, the Freundlich isotherm model assumes the multilayer adsorption with heterogeneity. It can be described as Eq. (4) [35]:

$$\ln Q = \ln K_F + \frac{1}{n} \ln C_e \quad (4)$$

Where C_e is the equilibrium concentration of metal ions in solution (mg L^{-1}), Q is the adsorbed value of metal ions at equilibrium concentration (mg g^{-1}), Q_0 and K_L is the Langmuir constants related to the adsorption capacity (mg g^{-1}) and energy of adsorption (L mg^{-1}), respectively. Plotting C_e/Q_e against C_e gives a straight line with slope and intercept equal to $1/Q_0$ and $1/(K_L Q_0)$, respectively. K_F (mol^{1-n} L^n g^{-1}) and n are Freundlich constants related to the adsorption capacity and adsorption intensity, respectively. The value of K_F represents the adsorption capacity when the equilibrium metal ion concentration equals to 1 and n represents the degree of dependence of the adsorption on the equilibrium concentration.

The fitting curves between the uptake Q_e and the equilibrium concentration of metals ions (C_e) by the Langmuir and Freundlich isotherms are shown in Fig. 4, and the various isotherm parameters are listed in Table 1. The adsorption of Pb(II) for GO and PAM-g-graphene is well fitted to the Langmuir isotherm model with the higher R^2 value. It indicates the adsorption process took place at specific homogeneous sites within GO and PAM-g-graphene which is regarded as monolayer adsorption. The theoretical maximum adsorption capacity, Q_0, determined by the Langmuir isotherm gives an adsorption capacity of GO and PAM-g-graphene for Pb(II) was 604 and 819.67 mg g^{-1}, respectively. The adsorption results suggested that the as-prepared PAM-g-graphene with PAM chains and little oxygen functional groups exhibits higher adsorption capacities of Pb(II) compared with GO. The strong adsorbability is attributed to the excellent properties of PAM-g-graphene such as water dispersibility and the functional groups on the PAM. Otherwise, the comparison of our adsorbent with some other sorbent materials for adsorption of Pb(II) is listed in Table 2 (Rt means room temperature). The adsorption capacities of PAM-g-graphene is 20 times and 8 times as strong as that of graphene nanosheets and carbon nanotubes, respectively. In previous work, Guixia Zhao et al. have demonstrated a kind of few-layered graphene oxide nanosheets, which have maximum adsorption capacities of Pb(II) ions calculated from the Langmuir model were about 842, 1150, and 1850 mg g^{-1} at 293, 313, and 333 K, respectively [33]. It's indicated that the maximum adsorption capacities for their few-layered graphene oxide nanosheets and our PAM-g-graphene at 293 K were approximate. However, the process time of adsorption achieved equilibrium for their samples was 24 h, which was much longer than our report in the present work (30 min). Consequently, this simple, novel and high efficient adsorbent for removal of Pb(II) from water has great prospect for industrial application.

Table 2
Comparison of maximum adsorption capacities for Pb(II) onto various adsorbents.

Adsorbent	Adsorption capacity (mg g^{-1})	Conditions		Reference
		pH	T (K)	
Graphene nanosheets	35.7	4	303	[29]
Graphite oxide	30.1	–	Rt	[46]
Carbon Nanotubes	102.4	5	Rt	[47]
Magnetic chitosan/graphene oxide	76.94	5	303	[28]
Functionalized graphene (GNS^{PF6})	405.9	5.1	Rt	[5]
Few-layered graphene oxide	842	6	293	[33]
Few-layered graphene oxide	1150	6	313	[33]
Few-layered graphene oxide	1850	6	333	[33]
LS-GO-PANI composite	216.4	5	303	[34]
SiO_2/graphene composite	113.6	6	298	[48]
PAM-g-graphene	819.67	6	293	This work
GO	604.00	6	293	This work

4. Conclusions

In summary, we prepared PAM-g-graphene directly from GO in aqueous by γ-ray simultaneously radiation with AM monomers at room temperature. The TGA results show that the degree of grafting of PAM-g-graphene sample is 24.2%, and the AFM results show that the thickness is measured to be 2.59 nm, which is higher than the pristine GO sheets. The experiment of absorption of Pb(II) on PAM-g-graphene indicates that the adsorption processes reach equilibrium in just 30 min and the maximum adsorption capacity of PAM-g-graphene is 819.67 mg g^{-1} which is 20 times and 8 times as strong as that of graphene nanosheets and carbon

nanotubes according to reports. This new type composite synthesized by this fast one-step approach, featuring a good versatility and adaptability, excellent adsorption capacity and rapid extraction, may provide a new idea for the global problem of heavy metal pollutants' removal in water.

Acknowledgments

The work was funded by the National Natural Science Foundation of China (11175130, U1362108) and China Postdoctoral Science Foundation (2014T70217).

Appendix A. Supplementary data

Supplementary data associated with this article can be found, in the online version, at http://dx.doi.org/10.1016/j.apsusc.2014.07.155.

References

[1] L.-Y. Meng, S.-J. Park, Preparation and characterization of reduced graphene nanosheets via pre-exfoliation of graphite flakes, Bull. Korean Chem. Soc. 33 (2012) 209–214.
[2] T.K. Das, S. Prusty, Graphene-based polymer composites and their applications, Polym. Plastics Technol. Eng. 52 (2013) 319–331.
[3] Y. Zhang, H.-L. Ma, Q. Zhang, J. Peng, J. Li, M. Zhai, Z.-Z. Yu, Facile synthesis of well-dispersed graphene by gamma-ray induced reduction of graphene oxide, J. Mater. Chem. 22 (2012) 13064–13069.
[4] B.W. Zhang, Y.J. Zhang, C. Peng, M. Yu, L.F. Li, B. Deng, P.F. Hu, C.H. Fan, J.Y. Li, Q. Huang, Preparation of polymer decorated graphene oxide by gamma-ray induced graft polymerization, Nanoscale 4 (2012) 1742–1748.
[5] X.J. Deng, L.L. Lv, H.W. Li, F. Luo, The adsorption properties of Pb(II) and Cd(II) on functionalized graphene prepared by electrolysis method, J. Hazard. Mater. 183 (2010).
[6] J.J. Yoo, K. Balakrishnan, J. Huang, V. Meunier, B.G. Sumpter, A. Srivastava, M. Conway, A.L.M. Reddy, J. Yu, R. Vajtai, P.M. Ajayan, Ultrathin planar graphene supercapacitors, Nano Lett. 11 (2011) 1423–1427.
[7] T. Kuilla, S. Bhadra, D. Yao, N.H. Kim, S. Bose, J.H. Lee, Recent advances in graphene based polymer composites, Prog. Polym. Sci. 35 (2010) 1350–1375.
[8] S. Yang, X. Feng, L. Wang, K. Tang, J. Maier, K. Mullen, Graphene-based nanosheets with a sandwich structure, Angew. Chem. Int. Ed. 49 (2010) 4795–4799.
[9] J.-H. Deng, X.-R. Zhang, G.-M. Zeng, J.-L. Gong, Q.-Y. Niu, J. Liang, Simultaneous removal of Cd(II) and ionic dyes from aqueous solution using magnetic graphene oxide nanocomposite as an adsorbent, Chem. Eng. J. 226 (2013) 189–200.
[10] J.R. Potts, D.R. Dreyer, C.W. Bielawski, R.S. Ruoff, Graphene-based polymer nanocomposites, Polymer 52 (2011) 5–25.
[11] S.B. Tapas Kuila, Ananta Kumar Mishra, Partha Khanra, Nam Hoon Kim, Joong Hee Lee, Chemical functionalization of graphene and its applications, Prog. Mater. Sci. 57 (2012).
[12] X.-D. Zhuang, Y. Chen, G. Liu, P.-P. Li, C.-X. Zhu, E.-T. Kang, K.-G. Neoh, B. Zhang, J.-H. Zhu, Y.-X. Li, Conjugated-polymer-functionalized graphene oxide: synthesis and nonvolatile rewritable memory effect, Adv. Mater. 22 (2010), 1731-+.
[13] D.R. Dreyer, S. Park, C.W. Bielawski, R.S. Ruoff, The chemistry of graphene oxide, Chem. Soc. Rev. 39 (2010) 228–240.
[14] X. Zhang, C. Cheng, J. Zhao, L. Ma, S. Sun, C. Zhao, Polyethersulfone enwrapped graphene oxide porous particles for water treatment, Chem. Eng. J. 215 (2013) 72–81.
[15] L. Chen, Z. Xu, J. Li, B. Zhou, M. Shan, Y. Li, L. Liu, B. Li, J. Niu, Modifying graphite oxide nanostructures in various media by high-energy irradiation, Rsc Adv. 4 (2014) 1025–1031.
[16] S.A. Vitusevich, V.A. Sydoruk, M.V. Petrychuk, B.A. Danilchenko, N. Klein, A. Offenhaeusser, A. Ural, G. Bosman, Transport properties of single-walled carbon nanotube transistors after gamma radiation treatment, J. Appl. Phys. 107 (2010).
[17] L. Chen, Z. Xu, J. Li, Y. Li, M. Shan, C. Wang, Z. Wang, Q. Guo, L. Liu, G. Chen, X. Qian, A facile strategy to prepare functionalized graphene via intercalation, grafting and self-exfoliation of graphite oxide (vol 22, pg 13460, 2012), J. Mater. Chem. 22 (2012) 25495.
[18] W.T. Wu, L. Shi, Y.S. Wang, W.M. Pang, Q.R. Zhu, One-step functionalization of multi-walled carbon nanotubes with Ag/polymer under gamma-ray irradiation, Nanotechnology 19 (2008).
[19] J.X. Guo, Y.G. Li, S.W. Wu, W.X. Li, The effects of gamma-irradiation dose on chemical modification of multi-walled carbon nanotubes, Nanotechnology 16 (2005) 2385–2388.
[20] S.M. Chen, G.Z. Wu, Y.D. Liu, D.W. Long, Preparation of poly(acrylic acid) grafted multiwalled carbon nanotubes by a two-step irradiation technique, Macromolecules 39 (2006) 330–334.
[21] B.W. Zhang, L. Li, Z. Wang, S. Xie, Y. Zhang, Y. Shen, M. Yu, B. Deng, Q. Huang, C. Fan, J. Li, Radiation induced reduction: an effective and clean route to synthesize functionalized graphene, J. Mater. Chem. 22 (2012) 7775–7781.
[22] D.S. Yang, D.J. Jung, S.H. Choi, One-step functionalization of multi-walled carbon nanotubes by radiation-induced graft polymerization and their application as enzyme-free biosensors, Radiat. Phys. Chem. 79 (2010) 434–440.
[23] S. Lee, H. Lee, J.H. Sim, D. Sohn, Graphene oxide/poly(acrylic acid) hydrogel by gamma-ray pre-irradiation on graphene oxide surface, Macromol. Res. 22 (2014) 165–172.
[24] I. Ali, New generation adsorbents for water treatment, Chem. Rev. (2012).
[25] N.M. Mubarak, J.N. Sahu, E.C. Abdullah, N.S. Jayakumar, Removal of heavy metals from wastewater using carbon nanotubes, Separat. Purif. Rev. 43 (2014) 311–338.
[26] S. Luo, X. Li, L. Chen, J. Chen, Y. Wan, C. Liu, Layer-by-layer strategy for adsorption capacity fattening of endophytic bacterial biomass for highly effective removal of heavy metals, Chem. Eng. J. 239 (2014) 312–321.
[27] I. Ali, Water treatment by adsorption columns: evaluation at ground level, Separat. Purif. Rev. 43 (2014) 175–205.
[28] C.L. Lulu Fan, Min Sun, Xiangjun Li, Huamin Qiu, Highly selective adsorption of lead ions by water-dispersible magnetic chitosan/graphene oxide composites, Colloids Surf. B: Biointerf. 103 (2013).
[29] Z.-H. Huang, X. Zheng, W. Lv, M. Wang, Q.-H. Yang, F. Kang, Adsorption of Lead(II) ions from aqueous solution on low-temperature exfoliated graphene nanosheets, Langmuir 27 (2011) 7558–7562.
[30] H. Wang, X.Z. Yuan, Y. Wu, H.J. Huang, G.M. Zeng, Y. Liu, X.L. Wang, N.B. Lin, Y. Qi, Adsorption characteristics and behaviors of graphene oxide for Zn(II) removal from aqueous solution, Appl. Surf. Sci. 279 (2013) 432–440.
[31] H. Wang, X.Z. Yuan, Y. Wu, H.J. Huang, X. Peng, G.M. Zeng, H. Zhong, J. Liang, M.M. Ren, Graphene-based materials: Fabrication, characterization and application for the decontamination of wastewater and wastegas and hydrogen storage/generation, Adv. Colloid Interf. Sci. 195 (2013) 19–40.
[32] S. Wang, H. Sun, H.M. Ang, M.O. Tade ; Adsorptive remediation of environmental pollutants using novel graphene-based nanomaterials, Chem. Eng. J. 226 (2013) 336–347.
[33] G.X. Zhao, X.M. Ren, X. Gao, X.L. Tan, J.X. Li, C.L. Chen, Y.Y. Huang, X.K. Wang, Removal of Pb(II) ions from aqueous solutions on few-layered graphene oxide nanosheets, Dalton Trans. 40 (2011) 10945–10952.
[34] J. Yang, J.-X. Wu, Q.-F. Lu, T.-T. Lin, Facile preparation of lignosulfonate-graphene oxide-polyaniline ternary nanocomposite as an effective adsorbent for Pb(II) ions, ACS Sustain. Chem. Eng. 2 (2014) 1203–1211.
[35] L. Liu, S.X. Liu, Q.P. Zhang, C. Li, C.L. Bao, X.T. Liu, P.F. Xiao, Adsorption of Au(III), Pd(II), and Pt(IV) from Aqueous Solution onto Graphene Oxide, J. Chem. Eng. Data 58 (2013) 209–216.
[36] V. Chandra, K.S. Kim, Highly selective adsorption of Hg2+ by a polypyrrole-reduced graphene oxide composite, Chem. Commun. 47 (2011) 3942–3944.
[37] S. Villar-Rodil, J.I. Paredes, A. Martinez-Alonso, J.M.D. Tascon, Preparation of graphene dispersions and graphene-polymer composites in organic media, J. Mater. Chem. 19 (2009) 3591–3593.
[38] D. Luo, G. Zhang, J. Liu, X. Sun, Evaluation criteria for reduced graphene oxide, J. Phys. Chem. C 115 (2011) 11327–11335.
[39] Q.R. Qixian Zhang, Yuqing Miao, Junhua Yuan, Kaikai Wang, Fenghua Li, Dongxue Han, Li Niu, One-step synthesisof graphene/polyallylamine–Au nanocomposites and their electrocatalysis toward oxygen reduction, Talanta 89 (2012).
[40] Y.-H. Yu, Y.-Y. Lin, C.-H. Lin, C.-C. Chan, Y.-C. Huang, High-performance polystyrene/graphene-based nanocomposites with excellent anti-corrosion properties, Polym. Chem. 5 (2014) 535–550.
[41] J. Shen, B. Yan, T. Li, Y. Long, N. Li, M. Ye, Study on graphene-oxide-based polyacrylamide composite hydrogels, Compos. Part a-Appl. Sci. Manuf. 43 (2012) 1476–1481.
[42] N.N. Zhang, R.Q. Li, L. Zhang, H.B. Chen, W.C. Wang, Y. Liu, T. Wu, X.D. Wang, W. Wang, Y. Li, Y. Zhao, J.P. Gao, Actuator materials based on graphene oxide/polyacrylamide composite hydrogels prepared by in situ polymerization, Soft Matter 7 (2011) 7231–7239.
[43] X. Mi, W. Xie, W. Wang, Y. Liu, J. Gao, Preparation of graphene oxide aerogel and its adsorption for Cu^{2+} ions, Carbon 50 (2012).
[44] S.-T. Yang, Y. Chang, A. Cao, Y. Liu, H. Wang, Removal of methylene blue from aqueous solution by graphene oxide, J. Colloid Interf. Sci. (2011) 24–29.
[45] H. Song, Y. Tian, X. Wan, L. Zhang, Y. Lv, Stable and water-dispersible graphene nanosheets: sustainable preparation, functionalization, and high-performance adsorbents for Pb2+, ChemPlusChem 77 (2012).
[46] O. Olanipekun, A. Oyefusi, G.M. Neelgund, A. Oki, Adsorption of lead over graphite oxide, Spectrochim. Acta Part a-Mol. Biomol. Spectrosc. 118 (2014) 857–860.
[47] N.A. Kabbashi, M.A. Atieh, A. Al-Mamun, M.E.S. Mirghami, M.D.Z. Alam, N. Yahya, Kinetic adsorption of application of carbon nanotubes for Pb(II) removal from aqueous solution, J. Environ. Sci.-China 21 (2009) 539–544.
[48] L.Y. Hao, H.J. Song, L.C. Zhang, X.Y. Wan, Y.R. Tang, Y. Lv, SiO_2/graphene composite for highly selective adsorption of Pb(II) ion, J. Colloid Interf. Sci. 369 (2012) 381–387.